AMERICAN SOCIETY of
GENE & CELL
THERAPY

# Long Non-coding RNA LINC00339 Stimulates Glioma Vasculogenic Mimicry Formation by Regulating the miR-539-5p/TWIST1/MMPs Axis

Junqing Guo,[1,2] Heng Cai,[3,4] Xiaobai Liu,[3,4] Jian Zheng,[3,4] Yunhui Liu,[3,4] Wei Gong,[1,2] Jiajia Chen,[1,2] Zhuo Xi,[3,4] and Yixue Xue[1,2]

[1]Department of Neurobiology, College of Basic Medicine, China Medical University, Shenyang 110122, People's Republic of China; [2]Key Laboratory of Cell Biology, Ministry of Public Health of China, and Key Laboratory of Medical Cell Biology, Ministry of Education of China, China Medical University, Shenyang 110122, People's Republic of China; [3]Department of Neurosurgery, Shengjing Hospital of China Medical University, Shenyang 110004, People's Republic of China; [4]Liaoning Research Center for Translational Medicine in Nervous System Disease, Shenyang 110004, People's Republic of China

**Glioma is recognized as a highly angiogenic malignant brain tumor. Vasculogenic mimicry (VM) greatly restricts the therapeutic effect of anti-angiogenic tumor therapy for glioma patients. However, the molecular mechanisms of VM formation in glioma remain unclear. Here, we demonstrated that LINC00339 was upregulated in glioma tissue as well as in glioma cell lines. The expression of LINC00339 in glioma tissues was positively correlated with glioma VM formation. Knockdown of LINC00339 inhibited glioma cell proliferation, migration, invasion, and tube formation, meanwhile downregulating the expression of VM-related molecular MMP-2 and MMP-14. Furthermore, knockdown of LINC00339 significantly increased the expression of miR-539-5p. Both bioinformatics and luciferase reporter assay revealed that LINC00339 regulated the above effects via binding to miR-539-5p. Besides, overexpression of miR-539-5p resulted in decreased expression of TWIST1, a transcription factor known to play an oncogenic role in glioma and identified as a direct target of miR-539-5p. TWIST1 upregulated the promoter activities of MMP-2 and MMP-14. The *in vivo* study showed that nude mice carrying tumors with knockdown of LINC00339 and overexpression of miR-539-5p exhibited the smallest tumor volume through inhibiting VM formation. In conclusion, LINC00339 may be used as a novel therapeutic target for VM formation in glioma.**

## INTRODUCTION

Glioma is the most angiogenic primary brain tumor characterized by microvascular proliferations.[1] At present, anti-angiogenic therapy is an important strategy to inhibit glioma progression.[2] However, it remains unsatisfactory, which might result from failing to inhibit vasculogenic mimicry (VM).[3] Therefore, apart from traditional anti-angiogenic therapy, investigation of anti-VM on the molecular biology level and whether it further inhibits glioma progression need to be addressed clearly.

In recent years, evidence has shown that anti-angiogenic therapy might elicit greater malignancy due to the increase of tumor adapta-

tion and invasion in hypoxic and ischemic environment.[4] Besides, anti-angiogenic therapy may relate to the hypoxic response and VM formation.[5] VM is characterized by non-endothelial tumor cells forming tubular structures in aggressive tumors. These structures have been proved in several malignant tumors, including glioma.[6] There is significant association between VM and glioma grades, and VM has been revealed to be involved in the proliferation, invasion, and metastasis of glioma.[7–9] Also, researchers have found that the existence of VM may provide nutrients to ensure that glioma cells grow in hypoxic and ischemic environment.[10,11] Therefore, destruction of VM may be a novel perspective for glioma treatment strategy. However, the molecular mechanisms involved in the regulation of VM in glioma process remain elusive so far.

Recently, various studies have demonstrated that lncRNA and miR-NAs play critical roles in the regulation of diverse cellular processes, including tumor development, differentiation, and angiogenesis.[12–14] So far, to our knowledge, there are only few reports about LINC00339 and miR-539-5p. Long intergenic non-coding RNA LINC00339 (also known as HSPC157) was only reported to be a candidate for the action of genetic variants on endometriosis risk.[15] Recently, miR-539-5p was reported to be downregulated in the lipopolysaccharide (LPS)-treated periodontal ligament cells (PDLCs) compared with the control group.[16] In addition, miR-539 was previously reported to be a tumor suppressor in some cancers, such as osteosarcoma and hepatocellular carcinoma.[17,18] The studies about LINC00339 and miR-539-5p in glioma and VM inhibition remain unconducted.

TWIST1 is a basic helix-loop-helix (bHLH) transcription factor that regulates embryonic morphogenesis.[19] TWIST1 is upregulated in various cancers, including glioma.[20,21] Further, overexpression of

TWIST1 has been shown to promote cell metastasis, survival, and angiogenesis.[22] In addition, it is known that TWIST1 opens nuclear membrane pores with the help of an accessory protein and enters the nucleus to regulate transcription of downstream genes that are involved in the process of VM.[23] In recent years, TWIST1 has been proven to be a crucial inducer for tumor epithelial-mesenchymal transition and participates in the process of VM in hepatocellular carcinoma[24] and large-cell lung cancer.[25] However, the role of TWIST1 in the process of VM in glioma has not been documented.

Matrix metalloproteinases (MMPs) are a family of zinc-binding endopeptidases and are reported to be involved in many physiological processes including tissue growth and regeneration, embryonic development, angiogenesis, apoptosis and nerve growth.[26,27] Among these MMPs, MMP-2 and MMP-14 (also known as membrane type 1-matrix metalloproteinase, MT1-MMP) are overexpressed in malignant glioma, and their expression levels correlate directly with the pathologic grades of glioma.[28] They are considered essential in tumor invasion and migration.[29,30] One of the mechanisms of glioma invasion is the activation of downstream targets, where MMP-14 activates proMMP-2 and indirectly MMP-2. The expression level of MMP-14 closely correlates with the expression level of MMP-2.[31,32] Moreover, MMPs showed a positive correlation with VM formation. In the final stage of the VM signaling pathway, expression, and activation of MMP-14 can converts proMMP-2 to active MMP-2. MMP-2 binding with the activated MMP-14 promoted the cleavage of the laminin5γ2 chain into promigratory γ2′ and γ2x fragments, which in turn stimulated the ability of migration and invasion of tumor cells. Simultaneously, it also formed the so-called lumens, which are the VM.[33] Therefore, we hypothesized that MMP-14 and MMP-2 have similar molecular mechanism in the process of VM in glioma.

In summary, the aim of this present study is to clarify the role and potential mechanism of LINC00339 in inhibiting VM and to determine whether miR-539-5p and transcription factors TWIST1 are involved in this process. These findings suggest a new strategy for the glioma therapy based on anti-VM in the future.

## RESULTS

### LINC00339 Expression Was Significantly Associated with VM in Glioma

First, we examined VM in low-grade glioma tissues (LGGTs), high-grade glioma tissues (HGGTs), and normal brain tissues (NBTs) by CD34-PAS. Representative VMs were positive for (periodic acid-schiff) PAS but negative for CD34. The anti-CD34 immunohistochemical staining identified the endothelium in tissue sections, resulting in a brown product. PAS staining was conducted to identify basement membrane-like structures between tumor cells that were highlighted pink. Sometimes, red blood cells can be observed in the hollows. To examine whether LINC00339 expression correlates with VM, we further measured the levels of LINC00339 in LGGTs, HGGTs, and NBTs by qRT-PCR. As shown in Figure 1A, VM was not found in NBTs. We also found that VM rarely existed in LGGTs. On the contrary, VM was very common in HGGTs. Subsequently, the

expression levels of LINC00339 in the above tissues were analyzed by qRT-PCR. As shown in Figure 1B, LINC00339 expression was significantly upregulated in LGGTs and HGGTs compared with NBTs. Moreover, LINC00339 expression was significantly upregulated in HGGTs compared with LGGTs. Also, we detected the expression levels of LINC00339 in glioma cell lines (U87 and U251) and NHAs (normal human astrocytes). LINC00339 expression was much higher in U87 and U251 than that in NHAs (Figure 1C). Therefore, these results indicated that LINC00339 expression was significantly associated with VM in glioma (Figure 1D).

### Knockdown of LINC00339 Inhibited VM Formation

To explore the possible functional role of LINC00339 in inhibiting VM, the stably transfected U87 and U251 cells silencing of LINC00339 were used in the subsequent experiments. The efficiencies were shown in Figure 2A.

To further elucidate the potential mechanisms in regulating VM, we then assessed the effects of LINC00339 knockdown on U87 and U251 cells proliferation, migration, invasion, and tube formation. As shown in Figure 2B, the viability of cells was inhibited in shLINC00339 groups compared with shNC groups. As shown in Figure 2C, the ability of tube formation of cells was suppressed in shLINC00339 groups compared with shNC groups. As shown in Figure 2D, the migration and invasion of cells were decreased in shLINC00339 groups compared with shNC groups. In addition, we also evaluated the expression of VM-related molecular MMP-2 and MMP-14. The results showed that knockdown of LINC00339 downregulated the protein expression of MMP-2 and MMP-14 (Figure 2E). Collectively, these results indicated that knockdown of LINC00339 could inhibit glioma VM.

### Overexpression of miR-539-5p Inhibited VM Formation

The expression levels of miR-539-5p in human glioma tissues and cell lines were analyzed by qRT-PCR. As shown in Figure 3A, miR-539-5p expression was significantly downregulated in LGGTs and HGGTs compared with NBTs, Moreover, miR-539-5p expression was significantly downregulated in HGGTs compared with LGGTs. Also, we detected the expression levels of miR-539-5p in glioma cell lines (U87 and U251) and NHA; miR-539-5p expression was much lower in U87 and U251 than in NHAs (Figure 3B). To better understand the functional role of miR-539-5p in regulating VM, qRT-PCR was applied to validate the efficiency of pre-miR-539-5p and anti-miR-539-5p. The high transfection efficacy of pre-miR-539-5p and anti-miR-539-5p could sustain 7 days from 2 days post-transfection. The transfected efficacy at 3 days post-transfection was shown in Figure 3C.

We then assessed the effects of miR-539-5p overexpression and inhibition on U87 and U251 cell proliferation, migration, invasion, and tube formation. As shown in Figure 3D, the viability of cells in pre-miR-539-5p groups were reduced compared with pre-NC groups, whereas cells in anti-miR-539-5p groups showed the opposite effect. In addition, the tube formation, migration, and invasion as well as the
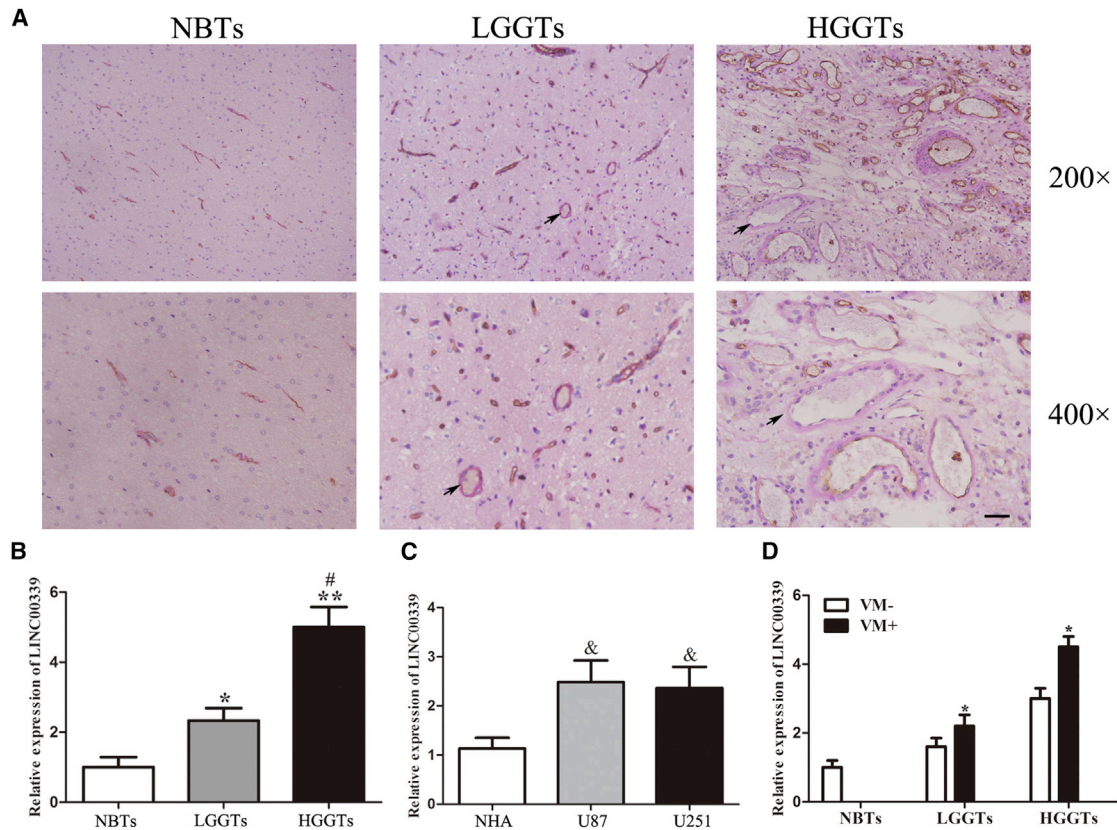
Figure 1. LINC00339 Expression Is Significantly Associated with VM in Glioma

(A) CD34-PAS double staining of normal brain tissues (NBTs), low-grade glioma tissues (LGGTs), and high-grade glioma tissues (HGGTs). VM is shown by black arrows (n = 3, NBT group; n = 10, each glioma tissue group) (magnification: top, 200× and bottom, 400×; scale bar, 50 μm). (B) Relative expression level of LINC00339 in NBTs, LGGTs, and HGGTs. Data represent means ± SD (n = 3, NBT group; n = 10, each glioma tissue group). *$p < 0.05$ versus NBT group. **$p < 0.01$ versus NBT group. #$p < 0.05$ versus LGGT group. (C) Relative expression level of LINC00339 in NHA, U87, and U251. Data represent means ± SD (n = 5, each). &$p < 0.05$ versus NHA group. (D) The correlation between VM and LINC00339 expression.

expression levels of MMP-2 and MMP-14 were similar to the above results (Figures 3E–3G).

### LINC000339 Negatively Regulated and Targeted miR-539-5p

LncRNA may function as a molecular sponge in modulating the expression and biological functions of miRNA.[34] As shown in Figure 4A, the expression level of miR-539-5p was significantly increased in stably transfected U87 and U251 cell silencing of LINC00339. To further clarify the underlying mechanism, bioinformatics prediction and luciferase reporter assays were performed (Figure 4B). The results showed no significant difference in the relative luciferase activity between co-transfection with LINC00339-Mut and pre-miR-539-5p groups and co-transfection with LINC00339-Mut and pre-NC groups; relative luciferase activity was markedly reduced in LINC00339-Wt and pre-miR-539-5p co-transfection groups compared with LINC00339-Wt and pre-NC co-transfection groups. To confirm whether LINC00339 and miR-539-5p were present in the expected RNA-induced silencing complex (RISC), an RNA-binding protein immunoprecipitation (RIP)

assay was carried out. qRT-PCR was performed to measure RNA levels in immunoprecipitates. The expression of LINC00339 and miR-539-5p were both increased in the anti-Ago2 group compared with the anti-normal group. In the anti-miR-539-5p group, the expressions of LINC00339 and miR-539-5p immunoprecipitated with Ago2 were lower than those in the control group, respectively (Figure 4C).

### LINC00339 Regulated VM via Binding to miR-539-5p

To clarify whether miR-539-5p was involved in the LINC00339-regulated VM, the combinations of transfection were conducted prior to the assessment of U87 and U251 cell proliferation, migration, invasion, and tube formation. As shown in Figure 5A, the results showed that the viability of U87 and U251 cells in shLINC00339 + pre-miR-539-5p groups was significantly decreased, while in shLINC00339 + anti-miR-539-5p groups, it was significantly increased. The tube formation, migration, and invasion as well as the expression of MMP-2 and MMP-14 were similar to the above results (Figures 5B–5D).
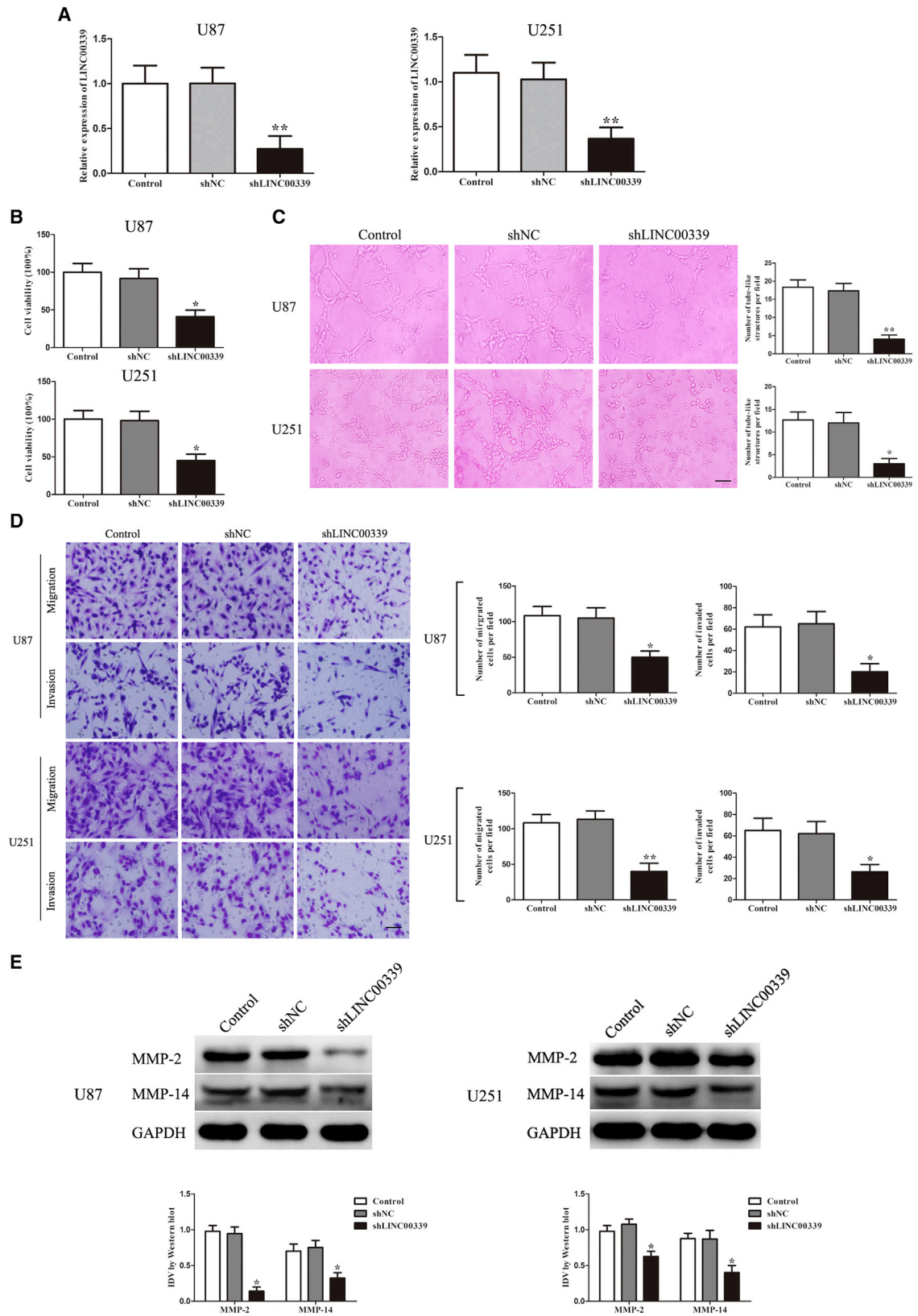
### MiR-539-5p Targeted and Negatively Regulated TWIST1

We assessed the effects of miR-539-5p overexpression and inhibition on the expression of TWIST1. Results showed that miR-539-5p overexpression decreased the protein expression of TWIST1, while miR-539-5p inhibition had the opposite effects (Figure 6A). The potential targets of miR-539-5p were predicted by the bioinformatics databases, and a luciferase reporter assay was performed (Figure 6B). The results showed no significant difference in the relative luciferase activity between the TWIST1-Mut + pre-miR-539-5p and TWIST1-Mut + pre-NC groups; the TWIST1-Wt + pre-miR-539-5p group significantly reduced luciferase activity compared with TWIST1-Wt + pre-NC group.

### TWIST1 Mediated the Tumor-Suppressive Effects of miR-539-5p-Regulated VM

To determine whether the tumor-suppressive effects of miR-539-5p-regulated VM were mediated by TWIST1, the combinations of transfection were conducted prior to the assessment of U87 and U251 cell proliferation, migration, invasion, and tube formation. As shown in Figure 7A, the results revealed that U87 and U251 cell viability in pre-miR-539-5p + TWIST1-NC groups was significantly decreased, while the viability in pre-miR-539-5p + TWIST1-ORF groups was significantly increased. In miR-539-5p + TWIST1-ORF-3′ UTR groups, the viability was decreased compared with that in miR-539-5p + TWIST1-ORF groups. The tube formation, migration, and invasion, as well as the expression of MMP-2 and MMP-14, were similar to the above results (Figures 7B–7D). Results revealed that miR-539-5p overexpression inhibited the proliferation, migration, invasion, and tube formation of U87 and U251 cells by targeting the 3′ UTR of TWIST1. TWIST1-ORF rescued the inhibitory effect induced by miR-539-5p overexpression. However, TWIST1-ORF-3′ UTR did not rescue the above effect.

### TWIST1 Bound to the Promoters of MMP-2 and MMP-14 Proteins in Glioma U87 and U251

We performed chromatin immunoprecipitation (ChIP) assays to clarify whether TWIST1 was directly associated with the promoters of MMP-2 and MMP-14 in U87 and U251. The position of transcription start site (TSS) of MMP-2 and MMP-14 was predicted by DBTSS HOME (http://dbtss.hgc.jp/). Analysis of sequences of upstream region (1,500 bp) and downstream region of the TSS using the "TFSEARCH" program indicated the presence of potential TWIST1-binding sites. Two putative TWIST1 binding sites at −285 and −281 positions in MMP-2 and two putative TWIST1 binding sites at −309 and −291 in MMP-14 were respectively confirmed. Primers were designed to bind sequences flanking the putative TWIST1 binding sites. As a negative control, PCR was conducted to amplify in the upstream region of the putative TWIST1 binding site that was not expected to associate with TWIST1, respectively. The results revealed that there was an association of TWIST1 with putative binding sites of MMP-2 and the putative binding site of MMP-14. There was no association of TWIST1 with all of the control regions (Figure 8).

### LINC00339 Knockdown Combined with miR-539-5p Overexpression Suppressed Tumor Growth and VM in a Xenograft Mouse Model

To further verify the above findings, in vivo xenograft mouse model was performed. As shown in Figure 9A, shLINC00339, pre-miR-539-5p, and shLINC00339 + pre-miR-539-5p groups had smaller tumor volumes compared with the shNC + pre-NC group, while shLINC00339 + pre-miR-539-5p group had the smallest tumor volume. As shown in Figure 9B, the survival analysis showed that shLINC00339, pre-miR-539-5p, and shLINC00339 + pre-miR-539-5p groups produced longer survival compared with the shNC + pre-NC group, while shLINC00339 + pre-miR-539-5p group demonstrated the longest survival. Last, we detected VM in vivo mouse xenograft model by CD34-PAS. As shown in Figure 9C, there was no significant difference in the number of VM between control and shNC + pre-NC group or in the number of VM of the shLINC00339, pre-miR-539-5p, and shLINC00339 + pre-miR-539-5p group. The shLINC00339 + pre-miR-539-5p group had the least number of VM.

### DISCUSSION

Glioma is recognized as a highly angiogenic tumor. It has been verified previously that anti-angiogenic tumor therapy is one of the therapeutic options for glioma patients.[35] But previous studies also confirmed that anti-angiogenic tumor therapy shows limited and transitory efficacy for glioma.[36] Endothelium-dependent vessels had been considered essential for supplying blood to tumor tissue. Conventional anti-angiogenic tumor therapy also relied on endothelial cells to regulate tumor angiogenesis. On other side, there is a fluid-conducting network that is formed by certain types of tumor cells through their acquisition of plasticity to mimic endothelial function.[37] Maniotis et al.[38] first reported that highly aggressive and metastatic melanoma cells formed a new vascular structure named vasculogenic mimicry. Subsequently, this tubular structure was found in various malignant tumors, including breast carcinoma,[39] ovarian carcinoma,[40] prostate carcinoma,[41] non-small-cell lung carcinomas,[42] and glioma.[43] In the present study, VM in the glioma tissues was determined by dual staining for endothelial marker CD34 and periodic acid-schiff. Our result demonstrated that the histologic grades of glioma tissues were positively correlated with glioma VM formation, which were consistent with previous studies.[43] Liu et al.[7]

---

**Figure 2. Knockdown of LINC00339 Inhibited VM Formation**

(A) Relative LINC00339 expression in U87 and U251 cells after transfection with LINC00339-silencing plasmid. (B) CCK-8 assay was used to evaluate the proliferation effect of LINC00339 on U87 and U251 cells. (C) Three-dimensional culture of U87 and U251 cells after LINC00339 knockdown was calculated (magnification, 100×; scale bar, 100 μm). (D) Migration and invasion of U87 and U251 cells after LINC00339 knockdown were measured (magnification, 200×; scale bar, 100 μm). (E) Western blot analysis was to evaluate the effect after LINC00339 knockdown on the protein expression of MMP-2 and MMP-14 in U87 and U251 cells. Data represent means ± SD (n = 5, each). *p < 0.05 versus shNC group. **p < 0.01 versus shNC group.
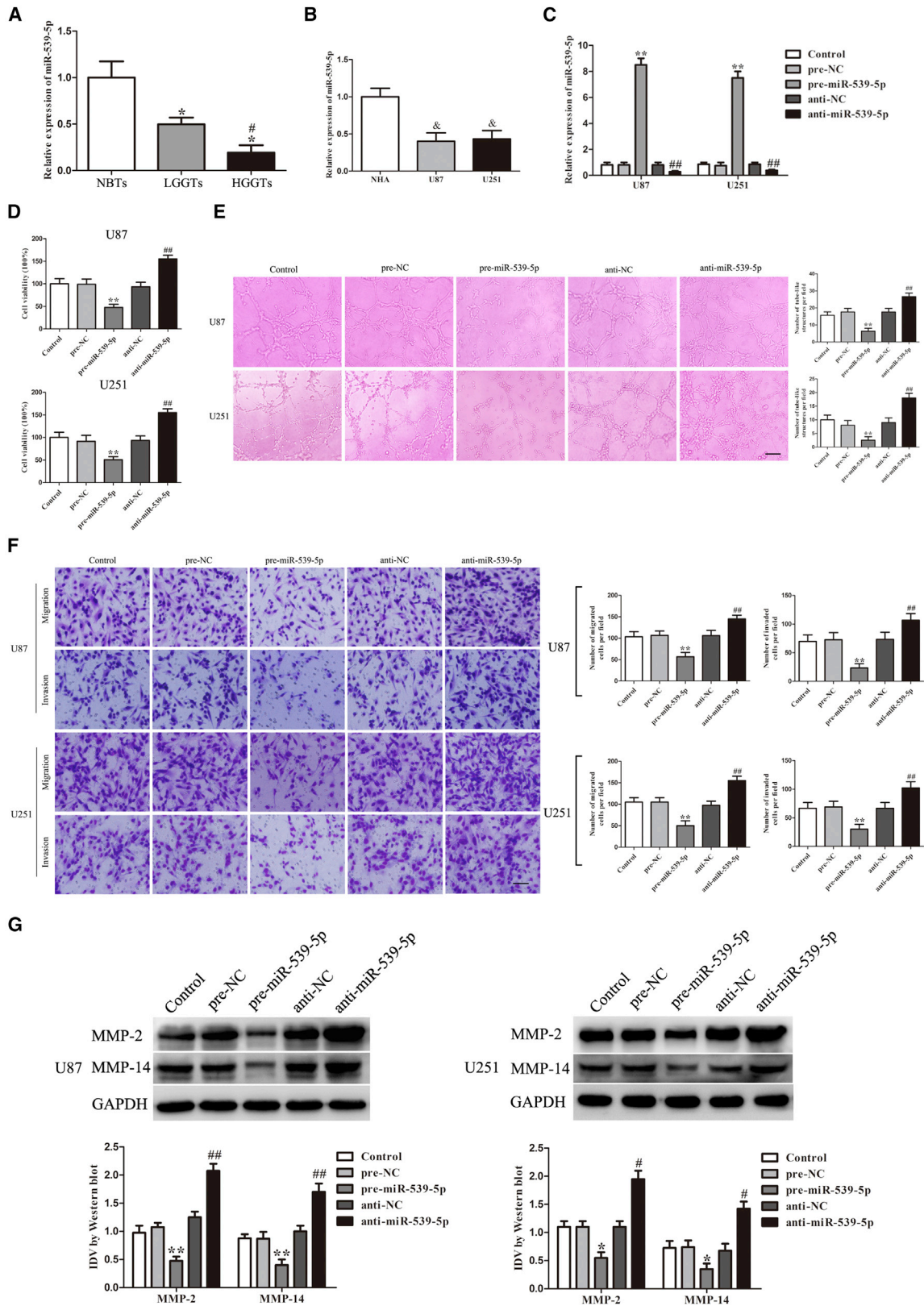
also detected the presence of VM in high-grade gliomas, and the high-histologic-grade glioma had a higher incidence of VM than that of lower-grade glioma. But the molecular mechanism of VM in glioma remains unclear.

Aberrant expression of some lncRNAs has been reported in glioma, and lots of lncRNAs played important roles in regulating biological processes of glioma. In the present study, we revealed for the first time that the expression of LINC00339 was significantly upregulated in glioma tissues as well as in glioma cells, suggesting that LINC00339 might be involved in the regulation of glioma progression. We also demonstrated that the expression levels of LINC00339 in glioma tissues were positively correlated with glioma VM formation. This evidence suggested that aberrant expression of LINC00339 might play a pivotal role in the glioma VM formation.

VM is characterized as a complex process that includes tumor cell proliferation, metastasis, invasion, as well as tube formation. In this work, we proved that LINC00339 expression in glioma cells was more upregulated than that in NHA cells. In an attempt to elucidate the effect of LINC00339 on glioma cells, we further investigated its possible role in regulating proliferation, metastasis, and invasion of glioma cells, which were critical for VM formation. The results showed that knockdown of LINC00339 inhibited the proliferation, migration, and invasion of glioma cells. Tube formation assay is recognized as a universal *in vitro* VM evaluation method.[44] Our results reflected that knockdown of LINC00339 impaired tube formation of glioma cells. Lots of factors were involved in glioma VM formation, including COX-2, VE-cadherin, TGF-β1, and so on. Previous studies also have indicated that the MMP family, especially MMP-2, MMP-9, and MMP-14, were involved in the key signaling pathway of VM formation.[45,46] Our results indicated that LINC00339 inhibited the expression of MMP-2 and MMP-14 in glioma cells. All the above results presented evidence that LINC00339 might be involved in regulation VM formation.

Recently, a new regulatory mechanism surfaced in which lncRNA might serve as a competing endogenous RNA (ceRNA) or a molecular sponge in modulating the expression and biological functions of miRNA,[34] suggesting that there might be an inverse correlation between expression of lncRNA and miRNA. In order to elucidate the molecular mechanism of LINC00339 in glioma VM formation, bioinformatics analysis and luciferase reporter assays were conducted to explore the potential targeted miRNA of LINC00339. The results

showed that LINC00339 might serve as a ceRNA in modulating the expression and biological functions of miR-539-5p. Our present study also showed that knockdown of LINC00339 significantly increased the expression of miR-539-5p in glioma cells. Moreover, we have validated the direct binding ability of the predicted miR-539-5p binding site on LINC00339. Previous studies have shown that some other lncRNAs serve as ceRNAs in modulating the expression of miR-539. For example, lncRNA CARL can act as an endogenous miR-539 sponge that regulates PHB2 expression, mitochondrial fission, and apoptosis.[47] LncRNA LOC100129148 enhanced the KLF12 expression through functioning as a competitive "sponge" for miR-539-5p in human nasopharyngeal carcinoma.[48]

MiR-539-5p was located at chromosome 14q32.31. This region has been characterized as a cancer suppressor gene in numerous cancers, including glioma. Our present study demonstrated that the endogenous expression of miR-539-5p was significantly downregulated in glioma tissues as well as in glioma cells, suggesting that it might be a tumor suppressor in glioma. Consistent with our results, miR-539-5p has been reported to exert a tumor-suppressive role in other cancers.[49] Our results showed that overexpression of miR-539-5p inhibited proliferation, migration, and invasion, impairing VM tube formation as well as downregulating the expression of MMP-2 and MMP-14 in glioma cells. On the contrary, knockdown of miR-539-5p remarkably promoted the proliferation, migration, and invasion of glioma cells as well as stimulated tube formation *in vitro*. Those findings indicated that miR-539-5p would be involved in VM formation and act as a tumor suppressor on VM formation. Furthermore, to investigate whether miR-539-5p mediated the suppressive effects of LINC00339 knockdown in glioma VM formation, LINC00339 knockdown combined with miR-539-5p overexpression inhibited VM *in vitro*. Moreover, the *in vivo* study showed that knockdown of LINC00339 combined with overexpression of miR-539-5p exhibited the smallest tumor volume as well as the longest survival and inhibited VM formation. Therefore, LINC00339 knockdown inhibited VM in glioma through upregulating miR-539-5p.

Accumulated evidence has shown that miRNAs can modulate biological processes by inhibiting protein translation and promoting the degradation of the target mRNAs by binding to the 3′ UTR of specific mRNAs.[50] A recent study indicated that miR-539-5p exerted its tumor-suppressive role on nasopharyngeal carcinoma by targeting KLF12.[48] In thyroid cancer, miR-539 inhibits cell migration and invasion by directly targeting CARMA1.[51] In osteosarcoma, miR-539

**Figure 3. Overexpression of miR-539-5p Inhibited VM Formation**

(A) Relative expression levels of miR-539-5p in NBTs, LGGTs, and HGGTs. Data represent means ± SD (n = 3, NBT group; n = 10, each glioma tissue group). *p < 0.05 versus NBT group. #p < 0.05 versus LGGT group. (B) Relative expression levels of miR-539-5p in NHA, U87, and U251. Data represent means ± SD (n = 5, each). &p < 0.05 versus NHA group. (C) Relative miR-539-5p expression in U87 and U251 cells after transfection with miR-539-5p agomir and miR-539-5p antagomir. (D) CCK-8 assay was used to evaluate the proliferation effect of miR-539-5p on U87 and U251 cells. (E) Three-dimensional culture of U87 and U251 cells with the expression of miR-539-5p changed was calculated (magnification, 100×; scale bar, 100 μm). (F) Migration and invasion of U87 and U251 cells with the expression of miR-539-5p changed were measured (magnification, 200×; scale bar, 100 μm). (G) Western blot analysis was to evaluate the effect with the expression of miR-539-5p changed on the protein expression of MMP-2 and MMP-14 in U87 and U251 cells. Data represent means ± SD (n = 5, each). *p < 0.05 versus pre-NC group. #p < 0.05 versus anti-NC group. **p < 0.01 versus pre-NC group. ##p < 0.01 versus anti-NC group.
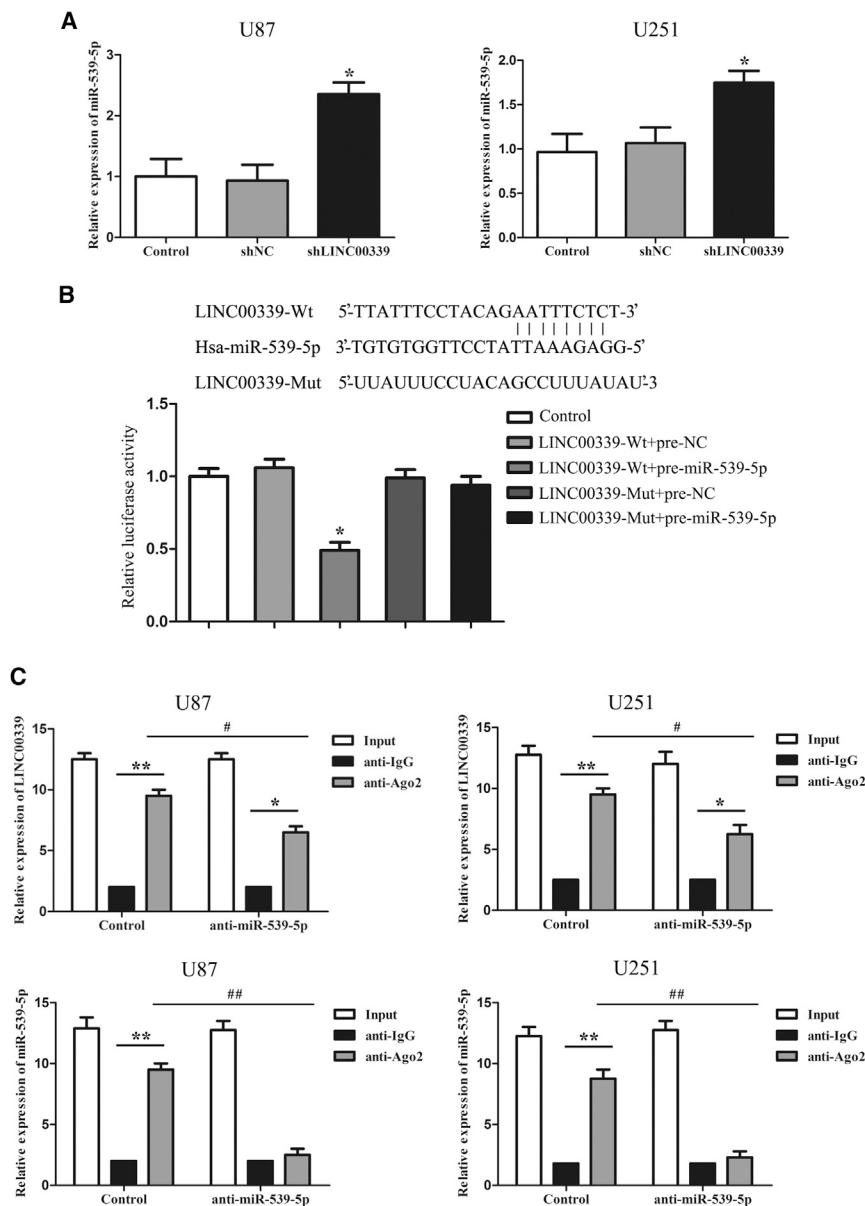
**A**



**B**

LINC00339-Wt      5'-TTATTTCCTACAGAATTTCTCT-3'
                              | | | | | | | | | |

Hsa-miR-539-5p   3'-TGTGTGGTTCCTATTAAAGAGG-5'

LINC00339-Mut    5'-UUAUUUCCUACAGCCUUUAUAU-3



**C**



**Figure 4. LINC000339 Negatively Regulated and Targeted miR-539-5p**

(A) Effect of knockdown of LINC00339 on the expression of miR-539-5p in U87 and U251 cells. Relative expression levels of miR-539-5p were detected by qRT-PCR. Data represent means ± SD (n = 3, each). *p < 0.05 versus shNC group. (B) Relative luciferase activity was performed by dual-luciferase reporter assay. Data represent means ± SD (n = 3, each). *p < 0.05 versus LINC00339-Wt + pre-NC group. (C) miR-539-5p was identified in LINC00339-RISC complex. LINC00339 and miR-539-5p expression levels were detected using qRT-PCR. Data represent means ± SD (n = 5, each). *p < 0.05 and **p < 0.01 versus anti-normal IgG group of respective group, #p < 0.05 and ##p < 0.01 versus anti-Ago2 in control group.

contributed to tumor cell plasticity and is strongly associated with VM formation. TWIST1 has been found to be a crucial inducer of epithelial mesenchymal transition.[55] Besides, it is known that TWIST1 opens nuclear membrane pores with the help of an accessory protein and enters the nucleus to regulate transcription of downstream genes that are involved in the process of VM formation. In hepatocellular carcinoma, TWIST1 not only plays an important role in tumor cell invasion and migration but was also closely associated with tumor cell plasticity to VM pattern.[56,57] In gastric cancer, MACC1 regulates TWIST1 and promotes VM formation.[58] To determine whether TWIST1 was involved in the miR-539-5p regulated VM formation, the combinations of transfection were conducted. The results showed that TWIST1-ORF could rescue the inhibitory effect induced by miR-539-5p overexpression, suggesting that TWIST1 could play an important role in miR-539-5p-mediated VM formation.
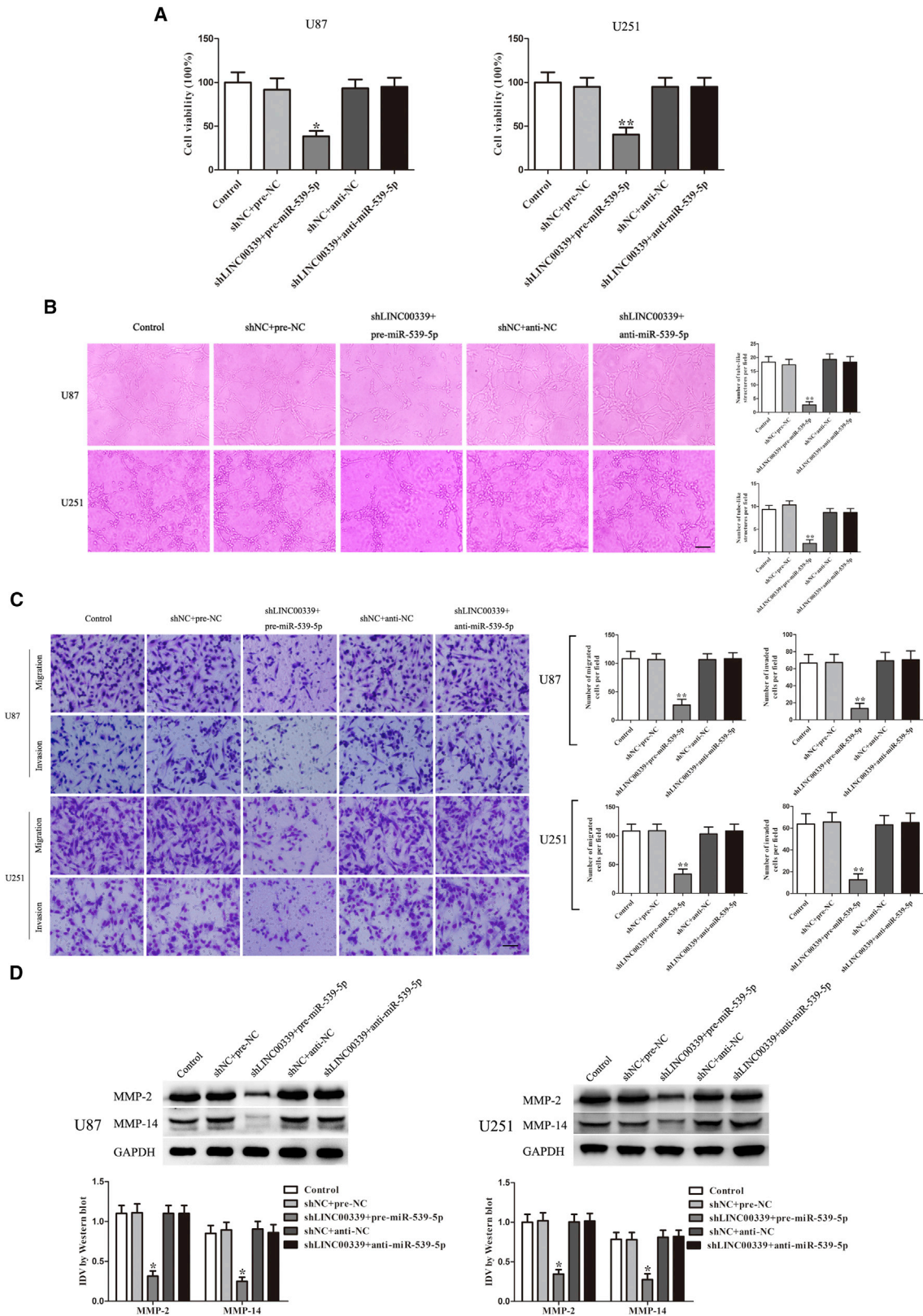
On the basis of these above findings, ChIP assays were performed to elucidate whether TWIST1 interacted with the promoters of MMP-2 and MMP-14. The results demonstrated that TWIST1 acted as a transcriptional factor, which could bind to the promoter region of MMP-2 and MMP-14. Previous reports had shown that TWIST1 interacted directly with the MMP-2 promoter to drive MMP-2 expression in glioma.[59]

## Conclusions

In conclusion, we discovered for the first time that the role of LINC00339 on glioma formation and the molecular mechanism of LINC00339 in affecting VM was correlated with the regulation of the miR-539-5p/TWIST1 pathway. Consequently, LINC00339 and related molecular pathways may be novel therapeutic targets for the inhibition of VM formation in glioma.

inhibits cell proliferation, invasion, and migration by targeting MMP-8.[52] In prostate cancer, ectopic overexpression of miR-539 can drastically inhibit SPAG5 expression, and the restoration of SPAG5 expression can reverse the inhibitory effects of miR-539 on cell proliferation and metastasis.[53] In our study, bioinformatics software and luciferase assays indicated that TWIST1 was the target of miR-539-5p. Overexpression of miR-539-5p reduced the expression of TWIST1, whereas the inhibition of miR-539-5p increased the secretion and expression of TWIST1. These results suggested that miR-539-5p inhibited the TWIST1 expression by targeting its 3′ UTR in glioma cells. TWIST1, a basic helix-loop-helix transcription factor, was revealed to play an oncogenic role in glioma and promoted invasion through epithelial-mesenchymal transition.[54] It
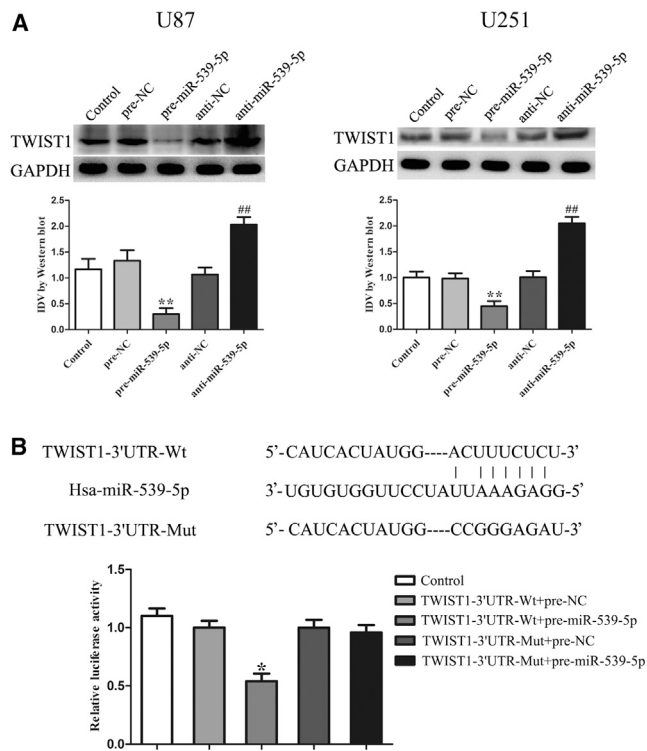
**Figure 6. miR-539-5p Targeted and Negatively Regulated TWIST1**

(A) The protein expression of TWIST1 after cells were transfected with miR-539-5p agomir and miR-539-5p antagomir. Data represent means ± SD (n = 3, each). **p < 0.01 versus pre-NC group. ##p < 0.01 versus anti-NC group. (B) Relative luciferase activity was performed by dual-luciferase reporter assay. Data represent means ± SD (n = 3, each). *p < 0.05 versus TWIST1-Wt + pre-NC group.

## MATERIALS AND METHODS

### Patient Tissue Specimens

All human glioma specimens and normal brain tissues (NBTs) were obtained from the Department of Neurosurgery, Shengjing Hospital of China Medical University. All tissues were immediately frozen in liquid nitrogen after surgical resection. The research procedures in our study were approved by the Institutional Review Board at the hospital. All participants provided their written informed consent and the hospital ethical committee approved the experiments. Glioma specimens were divided into two groups: low-grade glioma tissues (LGGTs) and high-grade glioma tissues (HGGTs) by at least two experienced neuropathologists according to the 2007 WHO classification of tumors in the central nervous system. NBTs were used as negative controls. The research protocol was reviewed and approved by the Ethics Committee of Shengjing Hospital of China Medical University, and informed consent was obtained from all

participants included in the study, in agreement with institutional guidelines.

### Cell Culture

Glioma U87 and U251 cell lines and HEK293T cells (Cell Resource Center, Shanghai Institutes for Biological Sciences) were cultured in high-glucose DMEM supplemented with 10% fetal bovine serum. Primary normal human astrocytes (NHA) were obtained from the Sciencell Research Laboratories (Carlsbad, CA, USA) and cultured in RPMI-1640 (Gibco, Carlsbad, CA, USA) with 10% fetal bovine serum. All the cells were incubated at 37°C in a humidified incubator with 5% $CO_2$ and changed medium every 2 days.

### CD34 Endothelial Marker Periodic Acid Schiff Dual Staining

CD34-PAS was examined for the presence of VM. First, standard immunohistochemical staining was performed with the help of UltraSensitive S-P kit (Fuzhou MaiXin Biotech, China). Formalin-fixed, paraffin-embedded tumor slides were cut at 5 μm, deparaffinized in xylene, hydrated, and boiled in EDTA antigen-unmasking solution. After slides were cooled to room temperature, incubated in peroxide at room temperature for endogenous peroxidase ablation, blocked with goat serum, and stained with a rabbit anti-human CD34 primary monoclonal antibody (1:100, Beijing Zhongshan Goldenbridge, China) overnight at 4°C. After washing with PBS thrice and incubating with goat-anti-rabbit secondary antibody at room temperature for 10 min, the slides were treated with a DAB kit (Fuzhou MaiXin Biotech, China). Then, the slides were exposed to periodic acid solution for 10 min, incubated with schiff solution for 10 min in dark, and counterstained with Mayer's hematoxylin (Zhuhai Baso, Guangdong, China). Lastly, the slides were viewed under a light microscope to detect CD34 and PAS signals.

### Quantitative Real-Time PCR Analysis

Total RNA was extracted from cells and tissues with the use of Trizol reagent according to the manufacturer's instructions (Life Technologies, Carlsbad, CA, USA). For measuring the expression level of LINC00339, 1 μg of RNA was reverse transcribed using a Primescript RT reagent kit with gDNA Eraser (Perfect Real Time) (TAKARA Bio Technology, Dalian, China) and quantitative real-time PCR was performed using SYBR Premix Ex TaqII (Tli RNaseH Plus) (TAKARA Bio Technology, Dalian, China). The information of LINC00339 and internal control GAPDH primers using as follows: LINC00339, forward, 5′-GGTTGACGAAGTCTGGA ACG-3′; reverse, 5′-GCCCATCATTTCATTGGGTA-3′; GAPDH, forward, 5′-GGTGAAGGTCGGAGTCAACG-3′; reverse, 5′-CCATG TAGTTGAGGTCAATGAAG-3′.

**Figure 5. LINC00339 Regulated Tumor-Induced VM via Binding to miR-539-5p**

(A) CCK-8 assay was used to evaluate the proliferation effect on U87 and U251 cells. (B) Three-dimensional culture of U87 and U251 cells was calculated (magnification, 100×; scale bar, 100 μm). (C) Migration and invasion of U87 and U251 cells were measured (magnification, 200×; scale bar, 100 μm). (D) Western blot analysis was to evaluate the effect on the protein expression of MMP-2 and MMP-14 in U87 and U251 cells. Data represent means ± SD (n = 5, each). *p < 0.05 versus shNC + pre-NC group. **p < 0.01 versus shNC + pre-NC group.
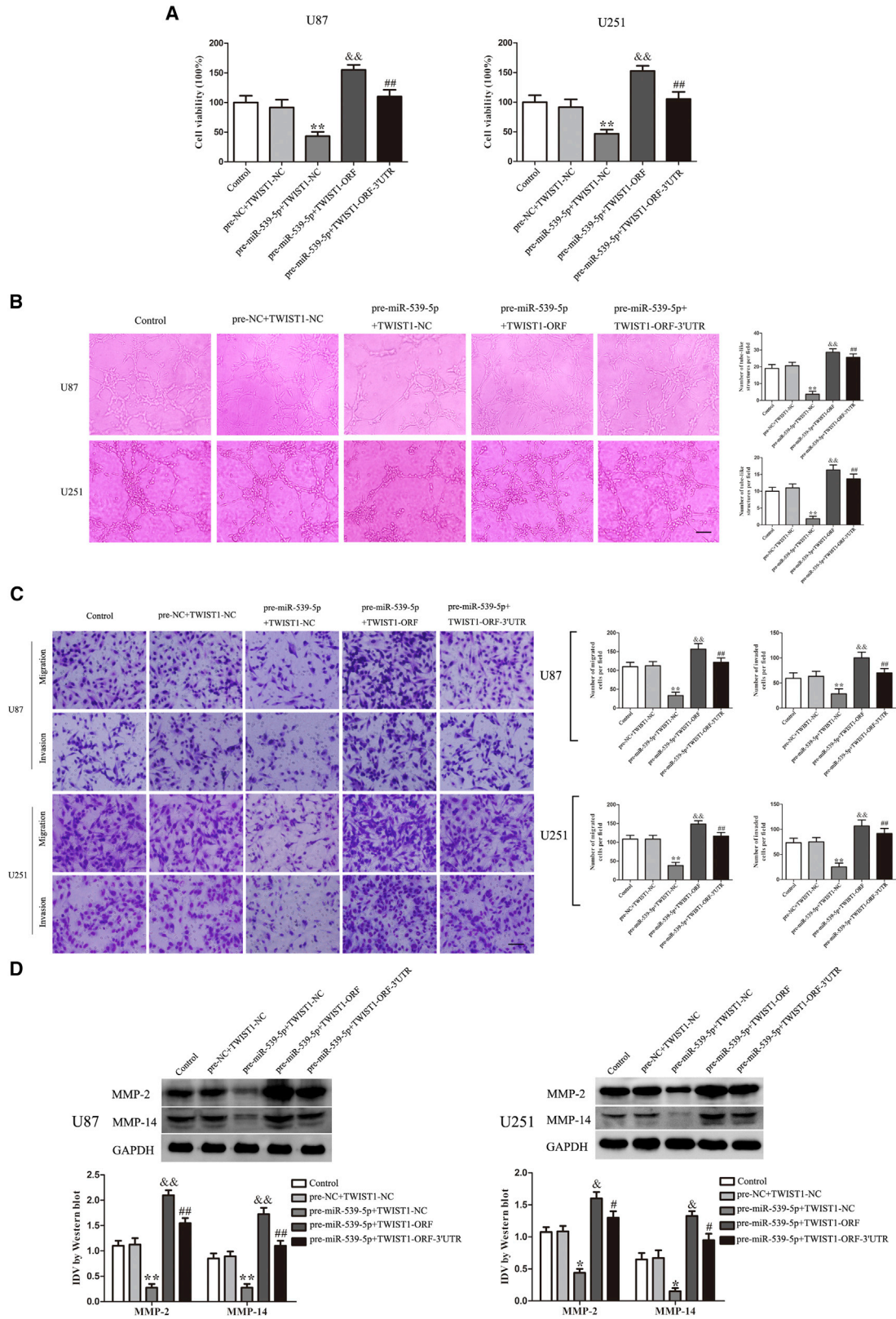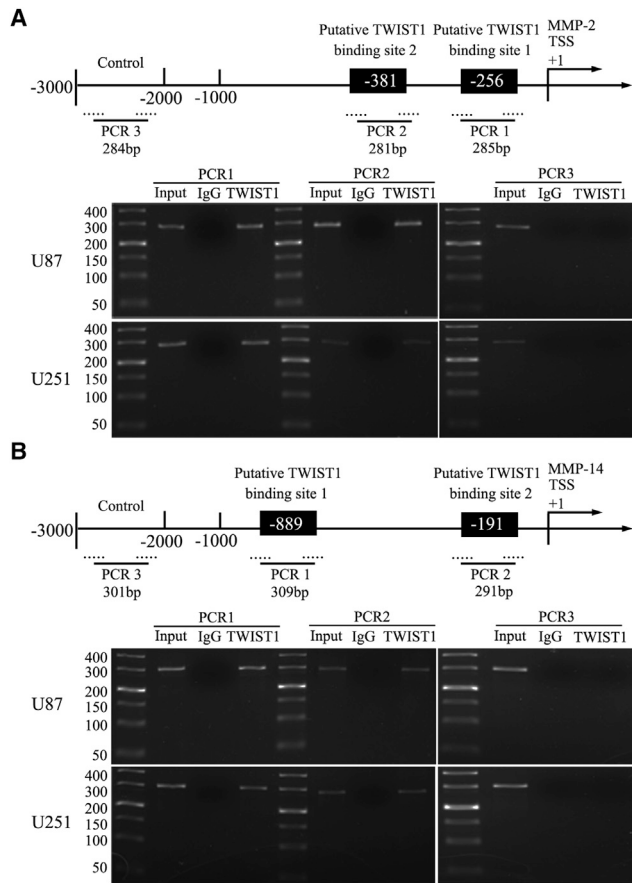
(legend on next page)

**Figure 8. TWIST1 Bound to the Promoters of MMP-2 and MMP-14 Proteins in Glima U87 and U251**

(A and B) Schematic representation of MMP-2 and MMP-14 promoter region in 3,000 bp upstream of the transcription start site (TSS, designated as +1). Chromatin immunoprecipitation (ChIP) PCR products for putative TWIST1 binding sites and an upstream region not expected to associate with TWIST1 are depicted with bold lines. Dashed lines represent the primers used for each PCR reaction. Image is representative of independent ChIP experiments (n = 3).

To test miR-539-5p expression, TaqMan MicroRNA Reverse Transcription Kits and Taqman Universal Master Mix II with the TaqMan MicroRNA Assay miR-539-5p and endogenous control U6 (Applied Biosystems, Foster City, CA, USA) were performed according to manufacturer's protocol. Relative levels of mRNA expression were analyzed using the quantification ($2^{-\Delta\Delta Ct}$) method.

### Transfection and Generation of Stably Transfected Cell Lines

Short-hairpin RNA directed against human LINC00339 was constructed in pGPU6/GFP/Neo plasmid (shLINC00339) (Gene Pharma, Shanghai, China). Human full-length TWIST1 coding sequence (CDS) and with its 3′ UTR sequences were ligated into pIRES2-EGFP plasmid (TWIST1-ORF and TWIST1-ORF-3′ UTR) (GenScript, Piscataway, NJ, USA), respectively. Plasmid carrying a non-targeting sequence was used as a negative control (NC).
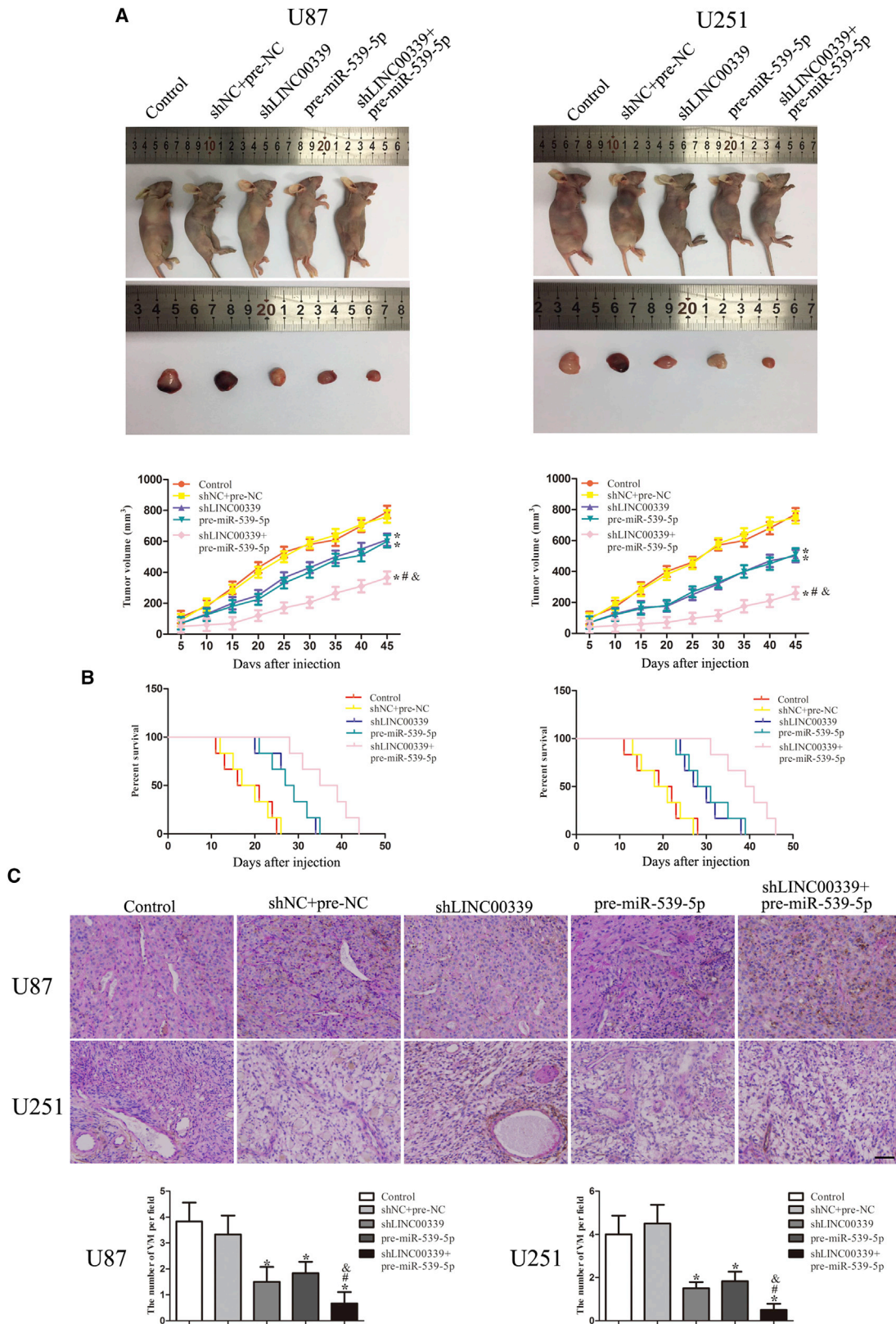
Transfection was performed at about 80% confluency of cells (glioma U87 and U251) in 24-well plates using Lipofectamine 3000 Reagents (Life Technologies, Carlsbad, CA, USA). The stably transfected cells were selected by the culture medium containing Geneticin (G418; Sigma-Aldrich, St. Louis, MO, USA). After approximately 4 weeks, G418-resistant cell clones were established. Stable cell lines transfected efficiencies were assessed by qRT-PCR.

### Transient Transfection of miRNAs and Grouping

MiR-539-5p agomir, miR-539-5p antagomir, and their respective non-targeting sequences (negative control, NC) were synthesized (Gene Pharma, Shanghai, China). Glioma U87 and U251 cells were respectively transfected with miR-539-5p agomir (pre-miR-539-5p), miR-539-5p antagomir (anti-miR-539-5p), or their respective NC using Lipofectamine 3000 reagent. The transfected efficacy was evaluated by qRT-PCR, and the high transfection efficacy occurred at second day after transfection; experiments were divided into five groups: control group, pre-NC group, pre-miR-539-5p group, anti-NC group, and anti-miR-539-5p group.

The shNC and shLINC00339 stable transfected cells co-transfected with miR-539-5p agomir, miR-539-5p antagomir, and their NC were divided into five groups: control group, shNC + pre-NC group (shNC stable transfected cells co-transfected with pre-NC), shLINC00339 + pre-miR-539-5p group (shLINC00339 stable transfected cells co-transfected with pre-miR-539-5p), shNC + anti-NC group (shNC stable transfected cells co-transfected with anti-NC), and shLINC00339 + anti-miR-539-5p group (shLINC00339 stable transfected cells co-transfected with anti-miR-539-5p).

The TWIST1-ORF and TWIST1-ORF-3′ UTR stable transfected cells co-transfected with miR-539-5p agomir or their NC were divided into five groups: control group (un-transfected cells), pre-NC + TWIST1-NC group (TWIST1-NC stable transfected cells co-transfected with pre-NC), pre-miR-539-5p + TWIST1-NC group (TWIST1-NC stable transfected cells co-transfected with

**Figure 7. TWIST1 Mediated the Tumor-Suppressive Effects of miR-539-5p-Regulated VM**

(A) CCK-8 assay was used to evaluate the proliferation effect on U87 and U251 cells. (B) Three-dimensional culture of U87 and U251 cells were calculated (magnification, 100×; scale bar, 100 μm). (C) Migration and invasion of U87 and U251 cells were measured (magnification, 200×; scale bar, 100 μm). (D) Western blot analysis was to evaluate the effect on the protein expression of MMP-2 and MMP-14 in U87 and U251 cells. Data represent means ± SD (n = 5, each). *p < 0.05 versus pre-NC + TWIST1-NC group. #p < 0.05 versus pre-miR-539-5p + TWIST1-NC group. &p < 0.05 versus pre-miR-539-5p + TWIST1-ORF group. **p < 0.01 versus pre-NC + TWIST1-NC group. ##p < 0.01 versus pre-miR-539-5p + TWIST1-NC group. &&p < 0.01 versus pre-miR-539-5p + TWIST1-ORF group.

**A**

U87

U251

**B**

**C**

*(legend on next page)*

pre-miR-539-5p), pre-miR-539-5p + TWIST1-ORF group (TWIST1-ORF stable transfected cells co-transfected with pre-miR-539-5p) and pre-miR-539-5p + TWIST1-ORF-3′ UTR group (TWIST1-ORF-3′ UTR stable transfected cells co-transfected with pre-miR-539-5p).

### Western Blot Analysis

Harvested cells (glioma U87 and U251) were lysed in cell lysis buffer (Beyotime Institute of Biotechnology, China) and whole-cell lysates (40 μg) were loaded onto SDS-PAGE and transferred to polyvinylidene difluoride (PVDF) membranes (Millipore, USA). The membranes were blocked with blocking buffer (5% non-fat milk in 1% Tween Tris-buffered saline [TBS]) for 2 hr at room temperature, followed by incubation with primary antibodies overnight at 4°C, incubated with horseradish peroxidase-conjugated secondary antibodies for 2 hr at room temperature and then developed with the enhanced chemiluminescence reagents (Beyotime Institute of Biotechnology, China) according to the manufacturer's protocol. For protein band analyses, an internal control GAPDH (Proteintech, USA) was used. The antibody against TWIST1, MMP-14, and MMP-2 was purchased from Proteintech.

### In vitro VM Tube Formation Assay

The formation of VM tube in glioma U87 and U251 cells was performed as described previously.[60] In brief, a 96-well culture plate was coated with 60 μL Matrigel Basement Membrane Matrix (BD Biosciences, Bedford, MA, USA) per well and then allowed to polymerize for 1 hr at 37°C. The cells were resuspended and seeded onto the surface of Matrigel at a density $1 \times 10^5$ cells/well, then incubated for 6 hr. The cell morphology and vascular structures were observed and photographed under an inverted microscope (Olympus, Tokyo, Japan). An independent observer counted the total number of tube-like structures per image.

### Cell Proliferation Assay

Cell proliferation assay was performed using the Cell Counting Kit-8 (CCK8, Beyotime Institute of Biotechnology, China) according to the instructions. Cells were plated into 96-well cell culture plates with five replicate wells for each group, 10 μL CCK8 was added into each well and incubated for another 4 hr; the optical density value of the samples were finally measured at the wavelength of 450 nm.

### Cell Migration and Invasion Assay

The abilities of cells to migrate and invade through a permeable membrane were assessed using the 24-well transwell chambers with 8-μm pore size polycarbonate membrane (Costar, Corning, NY, USA). The cells were resuspended in serum-free medium then seeded in the upper transwell chambers on the top side of membrane, or the upper chambers were pre-coated with Matrigel and incubated at 37°C for 4 hr before the invasion assay started, then the cells were incubated for about thirty hr at 37°C in a humidified incubator. The cells on the upper surface of the membrane were removed with cotton swabs; the migrated and invaded cells on the lower membrane surface were fixed with methanol and glacial acetic acid and then stained with 20% Giemsa solution for 30 min at room temperature. The number of cells that migrated and invaded through the membrane were counted in five random fields.

### Bioinformatics Prediction and Luciferase Reporter Assay

The potential miR-539-5p binding sites of LINC00339 were predicted with the help of bioinformatics databases (Starbase v2.0). The putative miR-539-5p target binding sequence in LINC00339 and its mutant of the binding sites were synthesized and cloned into the pmirGLO luciferase miRNA Target Expression vector (Promega, Madison, WI, USA).

The target genes of miR-539-5p were predicted using the bioinformatics databases miRanda (http://www.MiRanda.org). To examine whether miR-539-5p targets TWIST1 directly, we constructed wild-type TWIST1 reporter plasmid (TWIST1-Wt) and mutated-type TWIST1 reporter plasmid (TWIST1-Mut) with pmirGLO-promoter vector (GenePharma, Shanghai, China), respectively.

HEK293T cells were seeded in 96-well plates for 1 day, and cells at 60%–80% confluence were co-transfected with the pmirGLO vector constructed with either wild-type or mutation type and miR-539-5p overexpression or miRNA NC plasmids using Lipofectamine 3000 Reagents according to the manufacturer's instructions. The luciferase activity was measured 2 days after transfection using a dual luciferase assay kit (Promega, Madison, WI, USA), and the relative firefly luciferase activity was expressed as the ratio of firefly luciferase activity to renilla luciferase activity. All transfections were performed in triplicate.

### RNA Immunoprecipitation

RIP assay was performed using the EZ-Magna RIP Kit (Millipore, Billerica, MA, USA) according to the manufacturer's protocol. Glioma U87 and U251 cells lysates of the control groups and antago-mir-539-5p groups were prepared and incubated with RIP buffer containing magnetic beads conjugated with human anti-Argonaute2 (Ago2) antibody. Normal mouse immunoglobulin G (IgG) (Millipore) was regarded as negative control. Samples were incubated with Proteinase K buffer, and then immunoprecipitated RNA was isolated. The RNA concentration was measured by a Nanodrop (Thermo Scientific). Furthermore, purified RNA was obtained and analyzed by qRT-PCR.

**Figure 9. In Vivo Tumor Xenograft Study**
(A) For subcutaneous xenograft study, cells were injected subcutaneously into nude mice. A sample tumor from representative group was shown. Tumor volume was measured and calculated. (B) The survival curves of nude mice were shown. Data represent mean ± SD (n = 8, each). *p < 0.05 versus shNC + pre-NC group. #p < 0.05 versus shLINC00339 group. &p < 0.05 versus pre-miR-539-5p group. (C) CD34-PAS was applied to detect the VM in xenografted tumor, and results were expressed as the number of VM per field. (magnification, 400×; scale bar, 50 μm).

## ChIP Assay

ChIP was carried out with Simple ChIP Enzymatic Chromatin IP Kit (Cell Signaling Technology, Danvers, Massachusetts, USA) according to manufacturer's protocol. In brief, cells (glioma U87 and U251) were cross-linked with 1% formaldehyde in culture medium for 10 min and treated with glycine for 5 min at room temperature. These cells were collected in lysis buffer. Chromatin was then digested with Micrococcal Nuclease. Immunoprecipitation was incubated with anti-TWIST1 antibody (Proteintech, USA) or normal rabbit IgG followed by immunoprecipitation with Protein G Agarose beads during an overnight incubation at 4°C with gentle shaking. As an input reference, 2% were removed before antibody supplemental. The DNA cross-links was reversed by 5 mol/L NaCl and Proteinase K at 65°C for 2 hr, and then DNA was purified. Immunoprecipitated DNA was amplified by PCR using specific primers, the primers of each PCR set, and the sizes of PCR product. Immunoprecipitated DNA was amplified by PCR using their specific primers (MMP2, PCR1 (F) 5′-ACCATTCCTTCCCGTTCCT-3′, (R) 5′-CTACTCGCCCTCCTCCACTT-3′; PCR2 (F) 5′-TGAGCAGTGAGGATGACCAG-3′, (R) 5′-CACCTTGGGAAATAGAGCAGTC-3′; PCR3 (F) 5′-TTGGCCAGCTTCTTTACTGC-3′, (R) 5′-GGGTATCGGTTTCCAGTGTG-3′. MMP14, PCR1 (F) 5′-AGCTTTATCCTGCCCTCTCC-3′, (R) 5′-TCTGTGGCTCCAACCTTTGT-3′; PCR2 (F) 5′-GAGGAATCAAGCCACTCAGAA-3′, (R) 5′-TCTCTCGCTCTCTCCTCTGG-3′; PCR3 (F) 5′-TTTGCTGTCTCCCTCTGCTT-3′, (R) 5′-TTGGAAGTGGGCTCTTCAGT-3′). In each PCR reaction, the corresponding inputs were taken in parallel for PCR validation. The PCR products were resolved on a 3% agarose gel. Figure 8 is representative of three independent ChIP experiments.

## *In Vivo* Xenograft Mouse Model

For the *in vivo* study, the stably transfected cell lines (glioma U87 and U251 cells) were used. To generate pre-miR-539-5p and shLINC00339 + pre-miR-539-5p stably transfected cell lines, the plasmid pGCMV/EGFP/miR-539-5p (GenePharma) was transfected into cells, and the pGCMV/EGFP/miR-539-5p plasmids was transfected into shLINC00339 stable transfected cells using Lipofectamine 3000 reagent and selected by culture medium containing G418, respectively. Experiments were divided into five groups: control group, shNC + pre-NC group, shLINC00339 group, pre-miR-539-5p group, shLINC00339 + pre-miR-539-5p group.

The 4-week-old BALB/c athymic nude mice were obtained from the Cancer Institute of the Chinese Academy of Medical Science. Experiments with mice were conducted strictly in accordance with a protocol approved by the Administrative Panel on Laboratory Animal Care of the Shengjing Hospital. For subcutaneous implantation, $3 \times 10^5$ cells were injected subcutaneously into the flank area of each animal. Tumor volume was measured every 5 days and calculated by the following formula: volume (mm$^3$) 1/4 length width$^2$/2. For survival analysis in orthotopic inoculations, $3 \times 10^5$ cells were stereotactically implanted into the right striatum of the mice. The number of survived nude mice was recorded every 5 days for 45 days. Lastly, we detected VM *in vivo* mouse xenograft model by CD34-PAS.

## Statistical Analysis

All experiments were carried out at least three times. All data were expressed as the mean ± SD. Statistically significant differences between two groups were determined by Student's t test. For three or more groups, statistical analysis was performed using one-way ANOVA. $p < 0.05$ was considered as statistically significant.

## SUPPLEMENTAL INFORMATION

Supplemental Information includes eight figures and can be found with this article online at https://doi.org/10.1016/j.omtn.2017.11.011.

## AUTHOR CONTRIBUTIONS

J.G., H.C., and X.L. participated in the research design. J.G., H.C., X.L., J.Z., and W.G. conducted the experiments. W.G., J.C., Z.X., and H.C. contributed the new reagents or analytic tool. J.G., H.C., J.C., and J.Z. performed the data analysis. J.G., H.C., X.L., and Y.X. wrote or contributed to the writing of the manuscript. All authors read and approved the final manuscript.

## CONFLICTS OF INTEREST

The authors declare that they have no competing interests.

## ACKNOWLEDGMENTS

## REFERENCES

1. Louis, D.N., Ohgaki, H., Wiestler, O.D., Cavenee, W.K., Burger, P.C., Jouvet, A., Scheithauer, B.W., and Kleihues, P. (2007). The 2007 WHO classification of tumours of the central nervous system. Acta Neuropathol. *114*, 97–109.

2. Jain, R.K., di Tomaso, E., Duda, D.G., Loeffler, J.S., Sorensen, A.G., and Batchelor, T.T. (2007). Angiogenesis in brain tumours. Nat. Rev. Neurosci. *8*, 610–622.

3. van der Schaft, D.W., Seftor, R.E., Seftor, E.A., Hess, A.R., Gruman, L.M., Kirschmann, D.A., Yokoyama, Y., Griffioen, A.W., and Hendrix, M.J. (2004). Effects of angiogenesis inhibitors on vascular network formation by human endothelial and melanoma cells. J. Natl. Cancer Inst. *96*, 1473–1477.

4. Pàez-Ribes, M., Allen, E., Hudock, J., Takeda, T., Okuyama, H., Viñals, F., Inoue, M., Bergers, G., Hanahan, D., and Casanovas, O. (2009). Antiangiogenic therapy elicits malignant progression of tumors to increased local invasion and distant metastasis. Cancer Cell *15*, 220–231.

5. Xu, Y., Li, Q., Li, X.Y., Yang, Q.Y., Xu, W.W., and Liu, G.L. (2012). Short-term antivascular endothelial growth factor treatment elicits vasculogenic mimicry formation of tumors to accelerate metastasis. J. Exp. Clin. Cancer Res. *31*, 16.

6. Yue, W.Y., and Chen, Z.P. (2005). Does vasculogenic mimicry exist in astrocytoma? J. Histochem. Cytochem. *53*, 997–1002.

7. Liu, X.M., Zhang, Q.P., Mu, Y.G., Zhang, X.H., Sai, K., Pang, J.C., Ng, H.K., and Chen, Z.P. (2011). Clinical significance of vasculogenic mimicry in human gliomas. J. Neurooncol. *105*, 173–179.

8. Chen, Y., Jing, Z., Luo, C., Zhuang, M., Xia, J., Chen, Z., and Wang, Y. (2012). Vasculogenic mimicry-potential target for glioblastoma therapy: an in vitro and in vivo study. Med. Oncol. *29*, 324–331.

9. Wang, S.Y., Yu, L., Ling, G.Q., Xiao, S., Sun, X.L., Song, Z.H., Liu, Y.J., Jiang, X.D., Cai, Y.Q., and Ke, Y.Q. (2012). Vasculogenic mimicry and its clinical significance in medulloblastoma. Cancer Biol. Ther. *13*, 341–348.

10. Huang, M., Ke, Y., Sun, X., Yu, L., Yang, Z., Zhang, Y., Du, M., Wang, J., Liu, X., and Huang, S. (2014). Mammalian target of rapamycin signaling is involved in the vasculogenic mimicry of glioma via hypoxia-inducible factor-1α. Oncol. Rep. 32, 1973–1980.

11. Chen, Y.S., and Chen, Z.P. (2014). Vasculogenic mimicry: a novel target for glioma therapy. Chin. J. Cancer 33, 74–79.

12. Marshall, L., and White, R.J. (2008). Non-coding RNA production by RNA polymerase III is implicated in cancer. Nat. Rev. Cancer 8, 911–914.

13. Ling, H., Fabbri, M., and Calin, G.A. (2013). MicroRNAs and other non-coding RNAs as targets for anticancer drug development. Nat. Rev. Drug Discov. 12, 847–865.

14. Zhou, S., Ding, F., and Gu, X. (2016). Non-coding RNAs as emerging regulators of neural injury responses and regeneration. Neurosci. Bull. 32, 253–264.

15. Luong, H.T., Painter, J.N., Shakhbazov, K., Chapman, B., Henders, A.K., Powell, J.E., Nyholt, D.R., and Montgomery, G.W. (2013). Fine mapping of variants associated with endometriosis in the WNT4 region on chromosome 1p36. Int. J. Mol. Epidemiol. Genet. 4, 193–206.

16. Du, A., Zhao, S., Wan, L., Liu, T., Peng, Z., Zhou, Z., Liao, Z., and Fang, H. (2016). MicroRNA expression profile of human periodontal ligament cells under the influence of Porphyromonas gingivalis LPS. J. Cell. Mol. Med. 20, 1329–1338.

17. Mirghasemi, A., Taheriazam, A., Karbasy, S.H., Torkaman, A., Shakeri, M., Yahaghi, E., and Mokarizadeh, A. (2015). Retraction Note: Down-regulation of miR-133a and miR-539 are associated with unfavorable prognosis in patients suffering from osteosarcoma. Cancer Cell Int. 16, 84.

18. Zhu, C., Zhou, R., Zhou, Q., Chang, Y., and Jiang, M. (2016). microRNA-539 suppresses tumor growth and tumorigenesis and overcomes arsenic trioxide resistance in hepatocellular carcinoma. Life Sci. 166, 34–40.

19. Lee, M.S., Lowe, G.N., Strong, D.D., Wergedal, J.E., and Glackin, C.A. (1999). TWIST, a basic helix-loop-helix transcription factor, can regulate the human osteogenic lineage. J. Cell. Biochem. 75, 566–577.

20. Khan, M.A., Chen, H.C., Zhang, D., and Fu, J. (2013). Twist: a molecular target in cancer therapeutics. Tumour Biol. 34, 2497–2506.

21. Creighton, C.J., Gibbons, D.L., and Kurie, J.M. (2013). The role of epithelial-mesenchymal transition programming in invasion and metastasis: a clinical perspective. Cancer Manag. Res. 5, 187–195.

22. Cheng, G.Z., Zhang, W.Z., Sun, M., Wang, Q., Coppola, D., Mansour, M., Xu, L.M., Costanzo, C., Cheng, J.Q., and Wang, L.H. (2008). Twist is transcriptionally induced by activation of STAT3 and mediates STAT3 oncogenic function. J. Biol. Chem. 283, 14665–14673.

23. Valsesia-Wittmann, S., Magdeleine, M., Dupasquier, S., Garin, E., Jallas, A.C., Combaret, V., Krause, A., Leissner, P., and Puisieux, A. (2004). Oncogenic cooperation between H-Twist and N-Myc overrides failsafe programs in cancer cells. Cancer Cell 6, 625–630.

24. Sun, T., Sun, B.C., Zhao, X.L., Zhao, N., Dong, X.Y., Che, N., Yao, Z., Ma, Y.M., Gu, Q., Zong, W.K., and Liu, Z.Y. (2011). Promotion of tumor cell metastasis and vasculogenic mimicry by way of transcription coactivation by Bcl-2 and Twist1: a study of hepatocellular carcinoma. Hepatology 54, 1690–1706.

25. Li, Y., Sun, B., Zhao, X., Zhang, D., Wang, X., Zhu, D., Yang, Z., Qiu, Z., and Ban, X. (2015). Subpopulations of uPAR+ contribute to vasculogenic mimicry and metastasis in large cell lung cancer. Exp. Mol. Pathol. 98, 136–144.

26. Szabova, L., Son, M.Y., Shi, J., Sramko, M., Yamada, S.S., Swaim, W.D., Zerfas, P., Kahan, S., and Holmbeck, K. (2010). Membrane-type MMPs are indispensable for placental labyrinth formation and development. Blood 116, 5752–5761.

27. Sun, C., Wang, Q., Zhou, H., Yu, S., Simard, A.R., Kang, C., Li, Y., Kong, Y., An, T., Wen, Y., et al. (2013). Antisense MMP-9 RNA inhibits malignant glioma cell growth in vitro and in vivo. Neurosci. Bull. 29, 83–93.

28. Forsyth, P.A., Wong, H., Laing, T.D., Rewcastle, N.B., Morris, D.G., Muzik, H., Leco, K.J., Johnston, R.N., Brasher, P.M., Sutherland, G., and Edwards, D.R. (1999). Gelatinase-A (MMP-2), gelatinase-B (MMP-9) and membrane type matrix metalloproteinase-1 (MT1-MMP) are involved in different aspects of the pathophysiology of malignant gliomas. Br. J. Cancer 79, 1828–1835.

29. Li, H., Li, Z., Xu, Y.M., Wu, Y., Yu, K.K., Zhang, C., Ji, Y.H., Ding, G., and Chen, F.X. (2014). Epigallocatechin-3-gallate induces apoptosis, inhibits proliferation and decreases invasion of glioma cell. Neurosci. Bull. 30, 67–73.

30. Itoh, Y., and Seiki, M. (2006). MT1-MMP: a potent modifier of pericellular microenvironment. J. Cell. Physiol. 206, 1–8.

31. Bigg, H.F., Morrison, C.J., Butler, G.S., Bogoyevitch, M.A., Wang, Z., Soloway, P.D., and Overall, C.M. (2001). Tissue inhibitor of metalloproteinases-4 inhibits but does not support the activation of gelatinase A via efficient inhibition of membrane type 1-matrix metalloproteinase. Cancer Res. 61, 3610–3618.

32. Hur, J.H., Park, M.J., Park, I.C., Yi, D.H., Rhee, C.H., Hong, S.I., and Lee, S.H. (2000). Matrix metalloproteinases in human gliomas: activation of matrix metalloproteinase-2 (MMP-2) may be correlated with membrane-type-1 matrix metalloproteinase (MT1-MMP) expression. J. Korean Med. Sci. 15, 309–314.

33. Seftor, R.E., Seftor, E.A., Koshikawa, N., Meltzer, P.S., Gardner, L.M., Bilban, M., Stetler-Stevenson, W.G., Quaranta, V., and Hendrix, M.J. (2001). Cooperative interactions of laminin 5 gamma2 chain, matrix metalloproteinase-2, and membrane type-1-matrix/metalloproteinase are required for mimicry of embryonic vasculogenesis by aggressive melanoma. Cancer Res. 61, 6322–6327.

34. Cesana, M., Cacchiarelli, D., Legnini, I., Santini, T., Sthandier, O., Chinappi, M., Tramontano, A., and Bozzoni, I. (2011). A long noncoding RNA controls muscle differentiation by functioning as a competing endogenous RNA. Cell 147, 358–369.

35. Vredenburgh, J.J., Desjardins, A., Herndon, J.E., 2nd, Dowell, J.M., Reardon, D.A., Quinn, J.A., Rich, J.N., Sathornsumetee, S., Gururangan, S., Wagner, M., et al. (2007). Phase II trial of bevacizumab and irinotecan in recurrent malignant glioma. Clin. Cancer Res. 13, 1253–1259.

36. Ebos, J.M., Lee, C.R., Cruz-Munoz, W., Bjarnason, G.A., Christensen, J.G., and Kerbel, R.S. (2009). Accelerated metastasis after short-term treatment with a potent inhibitor of tumor angiogenesis. Cancer Cell 15, 232–239.

37. Hendrix, M.J., Seftor, E.A., Hess, A.R., and Seftor, R.E. (2003). Vasculogenic mimicry and tumour-cell plasticity: lessons from melanoma. Nat. Rev. Cancer 3, 411–421.

38. Maniotis, A.J., Folberg, R., Hess, A., Seftor, E.A., Gardner, L.M., Pe'er, J., Trent, J.M., Meltzer, P.S., and Hendrix, M.J. (1999). Vascular channel formation by human melanoma cells in vivo and in vitro: vasculogenic mimicry. Am. J. Pathol. 155, 739–752.

39. Shirakawa, K., Tsuda, H., Heike, Y., Kato, K., Asada, R., Inomata, M., Sasaki, H., Kasumi, F., Yoshimoto, M., Iwanaga, T., et al. (2001). Absence of endothelial cells, central necrosis, and fibrosis are associated with aggressive inflammatory breast cancer. Cancer Res. 61, 445–451.

40. Sood, A.K., Fletcher, M.S., Zahn, C.M., Gruman, L.M., Coffin, J.E., Seftor, E.A., and Hendrix, M.J. (2002). The clinical significance of tumor cell-lined vasculature in ovarian carcinoma: implications for anti-vasculogenic therapy. Cancer Biol. Ther. 1, 661–664.

41. Sharma, N., Seftor, R.E., Seftor, E.A., Gruman, L.M., Heidger, P.M., Jr., Cohen, M.B., Lubaroff, D.M., and Hendrix, M.J. (2002). Prostatic tumor cell plasticity involves cooperative interactions of distinct phenotypic subpopulations: role in vasculogenic mimicry. Prostate 50, 189–201.

42. Passalidou, E., Trivella, M., Singh, N., Ferguson, M., Hu, J., Cesario, A., Granone, P., Nicholson, A.G., Goldstraw, P., Ratcliffe, C., et al. (2002). Vascular phenotype in angiogenic and non-angiogenic lung non-small cell carcinomas. Br. J. Cancer 86, 244–249.

43. El Hallani, S., Boisselier, B., Peglion, F., Rousseau, A., Colin, C., Idbaih, A., Marie, Y., Mokhtari, K., Thomas, J.L., Eichmann, A., et al. (2010). A new alternative mechanism in glioblastoma vascularization: tubular vasculogenic mimicry. Brain 133, 973–982.

44. Lin, A.Y., Ai, Z., Lee, S.C., Bajcsy, P., Pe'er, J., Leach, L., Maniotis, A.J., and Folberg, R. (2007). Comparing vasculogenic mimicry with endothelial cell-lined vessels: techniques for 3D reconstruction and quantitative analysis of tissue components from archival paraffin blocks. Appl. Immunohistochem. Mol. Morphol. 15, 113–119.

45. Kirschmann, D.A., Seftor, E.A., Hardy, K.M., Seftor, R.E., and Hendrix, M.J. (2012). Molecular pathways: vasculogenic mimicry in tumor cells: diagnostic and therapeutic implications. Clin. Cancer Res. 18, 2726–2732.

46. Paulis, Y.W., Soetekouw, P.M., Verheul, H.M., Tjan-Heijnen, V.C., and Griffioen, A.W. (2010). Signalling pathways in vasculogenic mimicry. Biochim. Biophys. Acta 1806, 18–28.

47. Wang, K., Long, B., Zhou, L.Y., Liu, F., Zhou, Q.Y., Liu, C.Y., Fan, Y.Y., and Li, P.F. (2014). CARL lncRNA inhibits anoxia-induced mitochondrial fission and apoptosis in cardiomyocytes by impairing miR-539-dependent PHB2 downregulation. Nat. Commun. *5*, 3596.

48. Sun, K.Y., Peng, T., Chen, Z., Song, P., and Zhou, X.H. (2017). Long non-coding RNA LOC100129148 functions as an oncogene in human nasopharyngeal carcinoma by targeting miR-539-5p. Aging (Albany NY) *9*, 999–1011.

49. Lv, L.Y., Wang, Y.Z., Zhang, Q., Zang, H.R., and Wang, X.J. (2015). miR-539 induces cell cycle arrest in nasopharyngeal carcinoma by targeting cyclin-dependent kinase 4. Cell Biochem. Funct. *33*, 534–540.

50. Min, A., Zhu, C., Peng, S., Rajthala, S., Costea, D.E., and Sapkota, D. (2015). MicroRNAs as important players and biomarkers in oral carcinogenesis. BioMed Res. Int. *2015*, 186904.

51. Gu, L., and Sun, W. (2015). MiR-539 inhibits thyroid cancer cell migration and invasion by directly targeting CARMA1. Biochem. Biophys. Res. Commun. *464*, 1128–1133.

52. Jin, H., and Wang, W. (2015). MicroRNA-539 suppresses osteosarcoma cell invasion and migration in vitro and targeting Matrix metallopeptidase-8. Int. J. Clin. Exp. Pathol. *8*, 8075–8082.

53. Zhang, H., Li, S., Yang, X., Qiao, B., Zhang, Z., and Xu, Y. (2016). miR-539 inhibits prostate cancer progression by directly targeting SPAG5. J. Exp. Clin. Cancer Res. *35*, 60.

54. Mikheeva, S.A., Mikheev, A.M., Petit, A., Beyer, R., Oxford, R.G., Khorasani, L., Maxwell, J.P., Glackin, C.A., Wakimoto, H., González-Herrero, I., et al. (2010). TWIST1 promotes invasion through mesenchymal change in human glioblastoma. Mol. Cancer *9*, 194.

55. Kang, Y., and Massagué, J. (2004). Epithelial-mesenchymal transitions: twist in development and metastasis. Cell *118*, 277–279.

56. Sun, T., Zhao, N., Zhao, X.L., Gu, Q., Zhang, S.W., Che, N., Wang, X.H., Du, J., Liu, Y.X., and Sun, B.C. (2010). Expression and functional significance of Twist1 in hepatocellular carcinoma: its role in vasculogenic mimicry. Hepatology *51*, 545–556.

57. Ma, J.L., Han, S.X., Zhu, Q., Zhao, J., Zhang, D., Wang, L., and Lv, Y. (2011). Role of Twist in vasculogenic mimicry formation in hypoxic hepatocellular carcinoma cells in vitro. Biochem. Biophys. Res. Commun. *408*, 686–691.

58. Wang, L., Lin, L., Chen, X., Sun, L., Liao, Y., Huang, N., and Liao, W. (2015). Metastasis-associated in colon cancer-1 promotes vasculogenic mimicry in gastric cancer by upregulating TWIST1/2. Oncotarget *6*, 11492–11506.

59. Rahme, G.J., and Israel, M.A. (2015). Id4 suppresses MMP2-mediated invasion of glioblastoma-derived cells by direct inactivation of Twist1 function. Oncogene *34*, 53–62.

60. Francescone, R., Scully, S., Bentley, B., Yan, W., Taylor, S.L., Oh, D., Moral, L., and Shao, R. (2012). Glioblastoma-derived tumor cells induce vasculogenic mimicry through Flk-1 protein activation. J. Biol. Chem. *287*, 24821–24831.